Extremophiles (2008) 12:741–752
DOI 10.1007/s00792-008-0177-3

ORIGINAL PAPER

The extremely halophilic archaeon *Halobacterium salinarum* R1 responds to potassium limitation by expression of the K^+-transporting KdpFABC P-type ATPase and by a decrease in intracellular K^+

Henrik Strahl · Jörg-Christian Greie

Received: 19 February 2008 / Accepted: 11 June 2008 / Published online: 17 July 2008

Abstract *Halobacterium* species balance high external osmolality by the accumulation of almost equimolar amounts of KCl. Thus, steady K^+ supply is a vital prerequisite for life of these extreme halophiles. So far, K^+ is reported to enter the halobacterial cell only passively by use of potential-driven uniporters. However, the genome of both the extreme halophilic archaeon *Halobacterium* sp. NRC-1 and *H. salinarum* R1 comprises one single gene cluster containing the genes *kdpFABC* coding for homologs of the bacterial ATP-driven K^+ uptake system KdpFABC, together with an additional ORF so far annotated as *cat3* in *Halobacterium* sp. NRC-1 and as UspA protein in *H. salinarum* R1 (the ORF is only referred to as *cat3* in the following). Deletion of the *kdpFABCcat3* genes led to a reduced ability to grow under limiting K^+ concentrations, whereas real-time RT-PCR measurements revealed *cat3*-dependent high expression rates of the Kdp system in case of external K^+ depletion. Synthesis of the KdpFABC complex enables *H. salinarum* R1 to grow under extreme potassium-limiting conditions of >20 μM K^+. These results provide the first experimental evidence of an ATP-driven K^+ uptake system in *Halobacterium*. Moreover, *H. salinarum* R1 was shown to further adapt to K^+ limitation by a significant decrease of the intracellular K^+ level, which suggests a rather complex mechanism of K^+ homeostasis, in which the adaptation of cellular K^+ concentrations and the concomitant transcriptional regulation of genes coding for a high-affinity ATP-driven K^+ uptake system ensure the essential potassium supply under limiting conditions.

Keywords Haloarchaea · *Halobacterium* · Potassium uptake · KdpFABC · Cat3 · KdpQ

Abbreviations

BRE	Transcription factor B responsive element
FEP	Flame emission photometry
INR	Transcription initiation region
OD	Optical density
ORF	Open reading frame
RT	Reverse transcriptase
TFB	Transcription factor B
Usp	Universal stress protein
$\Delta\psi_{K+}$	Potassium potential
$\Delta\psi_m$	Membrane potential

Introduction

Obligate halophilic *Halobacterium* species are well-adapted to conditions of extremely high salt concentrations. Optimal growth of these haloarchaea occurs around 3.5–4.3 M NaCl. Unlike most other halophilic and halotolerant microorganisms, these halophilic Archaea do not rely on organic osmotic solutes to maintain the osmotic balance with the hypersaline medium (Oren 1999; Kokoeva et al. 2002; Roberts 2005). To balance the high external Na^+ concentration, K^+ is accumulated inside the

Communicated by F. Robb.

H. Strahl
Institute for Cell and Molecular Biosciences,
Newcastle University, Newcastle, UK

J.-C. Greie (✉)
Fachbereich Biologie/Chemie, Abteilung Mikrobiologie,
Universität Osnabrück, Barbarastr. 11,
49076 Osnabrück, Germany
e-mail: greie@biologie.uni-osnabrueck.de

cell in equimolar amounts, resulting in an osmotic equilibrium with the environment with no significant turgor pressure (Wagner et al. 1978; Lanyi et al. 1979). The major fraction of the K^+ gradient is hypothesized to be generated via a uniport system, through which K^+ enters the cell passively in accordance with the size of the membrane potential ($\Delta\psi_m$) (Wagner et al. 1978; Lanyi et al. 1979). Following the Nernst equation, passive K^+ uptake is feasible if the potential of the cation ($\Delta\psi_{K+}$) is equal to or less negative than $\Delta\psi_m$. As soon as $\Delta\psi_{K+}$ is more negative than $\Delta\psi_m$, K^+ transport has to be energized either by symport or antiport with other ions or by the hydrolysis of ATP (Oren 1999). As demonstrated in our study, *Halobacterium* species grow in the presence of limiting K^+ concentrations down to >20 μM. The resulting K^+ gradient of more than 100,000-fold cannot be solely established by potential-driven channel-mediated K^+ transport, even in case of a membrane potential of 280–300 mV generated by the action of bacteriorhodopsin (Michel and Oesterhelt 1980). Although ATP-dependent K^+ accumulation has previously been reported for *Haloferax volcanii*, another member of the family of Halobacteriaceae (Meury and Kohiyama 1989), this ATP dependency was attributed to its regulatory effect on the activity of a putative TrkAH homolog, which possibly serves as a K^+/H^+ symporter (Bakker 1993; Stumpe et al. 1996; Oren 1999). Thus, no experimental data have yet been reported for a possible primary ATP-driven uptake system supplying the cell with K^+ in case of low potential-driven facilitated diffusion rates. First theoretical evidence for such a system could be drawn from the genomic sequences of *Halobacterium* sp. NRC-1 (Ng et al. 2000) and *H. salinarum* R1 (Pfeiffer et al. 2008), which encode diverse homologs of active K^+ transporters. First, as expected, there are multiple copies of ORFs coding for homologs of the already proposed TrkAH system, a low-affinity K^+ transport complex, which is driven by $\Delta\psi_m$ (Nakamura et al. 1998). But second, a homolog of the bacterial ATP-driven KdpFABC complex can be found, which serves as an inducible, high-affinity K^+ transport system (Bramkamp et al. 2007; Greie and Altendorf 2007).

The KdpFABC complex has been reported in a variety of bacteria and belongs to the family of P-type ATPases, a group of ATP-driven transporters characterized by the formation of a phosphointermediate during the catalytic cycle and by the inhibition by *ortho*-vanadate (Palmgren and Axelsen 1998). In *Escherichia coli*, expression of the *kdpFABC* operon is induced in case of a NaCl-mediated osmotic upshock or by external K^+ limitation. Expression is under control of the regulatory proteins KdpD and KdpE, which constitute a typical sensor kinase/response regulator system (Jung and Altendorf 2002). In both *H. salinarum* sp. NRC-1 and *H. salinarum* R1, homologs of the bacterial *kdpD* and *kdpE* genes are absent in the genome. However, an additional ORF was found immediately downstream of the *kdpFABC* gene cluster, which is annotated as *cat3* (*kdpFABCcat3*) in *H. salinarum* sp. NRC-1 (Ng et al. 2000) and as UspA protein in *H. salinarum* R1 (Pfeiffer et al. 2008). For reasons of clarity, the ORF is referred to as *cat3* throughout the manuscript.

This study focuses on the analysis of the DNA sequence, deletion mutagenesis, and expression analysis of the halobacterial *kdpFABCcat3* genes together with the characterization of cellular adaptation of *H. salinarum* R1 to K^+-limiting conditions. The results provide the first direct experimental evidence of the functional expression of an inducible, ATP-driven high-affinity K^+ uptake system in *Halobacterium*. In addition, cells were shown to further adapt to K^+ limitation by a significant decrease in both the cytoplasmic potassium concentration as well as the cell volume. Thus, the current opinion of K^+ homeostasis of *H. salinarum* solely mediated via membrane potential-driven K^+ uniporters is obviously only one aspect of a more complex cellular machinery.

Materials and methods

Halobacterium salinarum strains, plasmids, media, and cultivation

The genotypes of *H. salinarum* R1 strains and plasmids used in this work are described in Tables 1 and 2. For growth curves and analyses of K^+ uptake as well as for quantitative RT-PCR, strains were grown in media as described in Kauri et al. (1990) with the following modifications: The total salt concentration was increased to 25% (w/v) according the growth requirements of *H. salinarum*. Potassium salts were substituted with sodium salts to obtain a K^+-free medium, whereas potassium was added as KCl in required concentrations of 1, 3, 5, 50 or 100 mM. Casamino acids 0.5% (w/v) was used as carbon source. Although not explicitly specified for the growth of *Halobacterium*, this medium is suitable for haloarchaea in general and was used due to the lack of a standard *Halobacterium* growth medium. For transformation, knock-out mutagenesis, and non-quantitative RT-PCR, strains were grown in rich media as described for *Halobacterium* sp. NRC-1 (American Type Culture Collection medium 2185). If indicated, media were supplemented with 20 μg mL^{-1} of Simvastatin, which was extracted from solid tablets (Ratiopharm) with ethanol. All strains were grown under illumination with shaking at 37°C. Optical densities were followed at 600 nm by use of an UVIKON 943 double beam UV/Vis spectralphotometer.

For the complementation of a chromosomal *kdpFABCcat3* deletion with plasmid-encoded *kdpFABCcat3* or

Table 1 Archaeal strains

Strains	Genotype	Characteristics	Reference
H. salinarum R1	Wild-type	Gas vesicle deficient	Stoeckenius and Kunau (1968)
H. salinarum R1 Δ*kdpFABCcat3*	Δ*kdpFABCcat3*	Deletion of *kdpFABCcat3*	This study
H. salinarum R1 Δ*kdpFABC*	Δ*kdpFABC*	Deletion of *KdpFABC*; *cat3* expressed by $kdpF_P$	This study

Table 2 Plasmids

Plasmids	Genotype	Characteristics	Reference
pMKK100	Ap^R, Mv^R, *bgaH, Col*E1	*Halobacterium*/E. *coli* shuttle vector	Koch and Oesterhelt (2005)
pHJS1	Ap^R, Me^R, *bgaH, Col*E1 *kdpFABCcat3*	Plasmid-encoded expression of *kdpFABCcat3*	This study
pHJS2	Ap^R, Mv^R, *bgaH, Col*E1 *kdpFABC*	Plasmid-encoded expression of *kdpFABC*	This study
pHJS3	Ap^R, Mv^R, *bgaH, Col*E1	Knock-out plasmid for Δ*kdpFABC*	This study
pHJS4	Ap^R, Mv^R, *bgaH, Col*E1	Knock-out plasmid for Δ*kdpFABCcat3*	This study
pBAD24	Ap^R, *Col*E1	*E. coli* expression vector	Guzman et al. (1995)

Ap^R ampicillin resistance, Mv^R, mevinolin/simvastatin resistance

KdpFABC, strains and plasmids were constructed as described below. Freshly transformed cells were cultured in parallel in media initially containing 3 mM or 100 mM KCl for 8 days as described above.

Measurements of medium and cellular K^+ concentrations and cell volume

The concentration of K^+ in the growth medium was measured by FEP using an Eppendorf ELEX 6361 flame photometer in a buffer containing 5 mM CsCl and 1.5% (w/v) trichloroacetic acid. The amount of cytoplasmic K^+ was determined after centrifugation of 1 mL of culture and subsequent cell lysis in 1 mL ddH_2O by FEP as described above. In this context, the residual K^+ outside the cell can be neglected, since the K^+ content of the medium is far below the intracellular K^+ level. This is further demonstrated by the observation that an additional washing step with potassium-free medium salt solution prior to cell lysis had no effect on the values obtained. Cell volume was determined by conversion of cells into spheroplasts as described in Cline et al. (1989) followed by micrographic imaging using a Zeiss Axioskop 40 FL microscope with an attached CCD camera (Diagnostic Instruments SPOT RT Slider). The pixel area of 500 individual cells per sample (ten frames evaluated with 50 cells each) was captured and determined by use of the ImageJ V1.37 picture processing program. Image frames were calibrated by use of a microscopy calibration slide (Motic) as well as a flow cytometry size calibration kit (Molecular Probes) as size standards. The determined pixel area was finally converted into metric units. Cell volumes were calculated based on the assumption that spheroplasts form round non-expandable spheres, since the presence of stretch-activated mechanosensitive channels should prevent any increase in spheroplast size due to the mild osmotic downshock. Thus, the spheroplast volume represents the actual cell volume and is, therefore, referred to as cell volume. Total cell counts were assigned by use of a Neubauer (Marienfeld, Germany) haemocytometer. In any case, photographs were taken at four focal planes for each section photographed to account for spatial depth of the specimen. In addition, edge sharpness was included as filter criterion in automated pixel area recognition.

Cloning of the *kdpFABCcat3* genes, construction of plasmids, transformation, and knock-out mutagenesis

Genomic DNA of *H. salinarum* R1 was isolated by phenol/chloroform extraction followed by ethanol precipitation as described in Sambrook et al. (2001). A 6,735-bp genomic fragment carrying the *kdpFABCcat3* genes was isolated via PCR using Herculase enhanced DNA polymerase (Stratagene) together with primers 1 and 2 (Table 3). The resulting PCR product was cloned into pCR2.1-TOPO by use of the TOPO TA cloning kit (Invitrogen). A 5,914-bp *Eco*RV/*Xba*I restriction fragment of pCR2.1-TOPO carrying the *kdpFABCcat3* genes was then subcloned in pBAD24 using *Sma*I/*Xba*I restriction sites. Using the restriction sites *Nco*I and *Hin*dIII of the pBAD24 multi cloning site, a 5,944-bp *Nco*I/*Hin*dIII fragment carrying the *kdpFABCcat3* genes was subsequently cloned in pMKK100, finally resulting in plasmid pHJS1.

The plasmid carrying the *kdpFABC* genes without the *cat3* gene was constructed by two-step PCR with Herculase enhanced DNA polymerase by use of primers 2, 3, 4, and 5

Table 3 Primers

Primer	Sequence	Purpose
# 1	CTCGGAGGAGTGAGGGATTCGACGACCC	Cloning of the *kdpFABCcat3* genes
# 2	GACTTCTTGTGCAACGGACATCCACCGG	Cloning of the *kdpFABCcat3* genes
# 3	CGACGCCCACATTTCCCCGGCG	Deletion of *cat3*
# 4	GTCACGGCGGCCCTTAGTGGTCACCGTTCGCTATTTCG	Deletion of *cat3*
# 5	CGGTGACCACTAAGGGCCGCCGTGACAGACTCA	Deletion of *cat3*
# 6	GCCCACCTCAGCCTCGTGCGCGCCATGGGCAGC	Δ*kdpFABC*/Δ*kdpFABCcat3*
# 7	GTTTCGTGCTGACATGTGCAACTGGCCCGGATGATTTC	Δ*kdpFABC*
# 8	CGGGCCAGTTGCACATGTCAGCACGAAACGAAACCGG	Δ*kdpFABC*
# 9	GCGCGAAGCTTGACGACCACTGGCACCAGTATC	Δ*kdpFABC*/Δ*kdpFABCcat3*
# 10	GGTCACGGCGGCCCCATGTGCAACTGGCCCGGATGATTTC	Δ*kdpFABCcat3*
# 11	CGGGCCAGTTGCACGGGCCGCCGTGACCGCCTCAC	Δ*kdpFABCcat3*
# 12	CGACGCCCACATTTCCCCGGCG	Real time RT-PCR *kdpC*/*cat3*
# 13	GTCTACGAGGATGCTCGACAGCTC	Real time RT-PCR *kdpC*/*cat3*
# 14	CGGGCGGCTGCAACGGCCAC	Real time RT-PCR *rpoA1*
# 15	CATCGACGCCGCGATGCGCTC	Real time RT-PCR *rpoA1*
# 16	CCTGGAAAGGGTACCTAAAGGCGG	Real time RT-PCR *kdpA*
# 17	GTCTACGAGGATGCTCGACAGCTC	Real time RT-PCR *kdpA*

(Table 3). The resulting PCR product was subcloned into the pBAD24 derivative carrying the *kdpFABCcat3* genes described above using the *Apa*I/*Xba*I restriction sites. An *Nco*I/*Hin*dIII fragment carrying *kdpFABC* genes was subsequently cloned in pMKK100 resulting in plasmid pHJS2.

Plasmids used for the knock-out mutagenesis of chromosomally encoded *kdpFABCcat3* and *kdpFABC* were constructed by two-step PCR technique using Herculase enhanced DNA polymerase and primers 6, 7, 8, 9, 10, and 11 (Table 3). The resulting PCR products carrying two 450-bp sequences framing the *kdpFABC* and *kdpFABCcat3* genes were cloned in plasmid pMKK100 by use of the restriction sites *Nco*I and *Hin*dIII, resulting in plasmids pHJS3 and pHJS4, respectively.

Transformation of *H. salinarum* R1 was done according to Cline et al. (1989). Knock-out mutagenesis by recombination for the deletion of *kdpFABC* and *kdpFABCcat3* in *H. salinarum* R1 was conducted by use of the knock-out plasmids pHJS3 and pHJS4, respectively, as described in Krebs et al. (1993). Deletion of the *kdpFABC* and *kdpFABCcat3* genes was controlled by PCR. In addition, the absence of expression was confirmed by RT-PCR.

RNA extraction, RT-PCR, and real time RT-PCR

Total RNA of *H. salinarum* R1 was isolated from cultures grown in either rich medium or in casaminoacids medium with varying K^+ concentrations by use of the RNeasy mini kit (Qiagen) following the manufacturer's instructions. RNA was diluted to a concentration of 20 μg mL^{-1} and subsequently treated with DNaseI (Fermentas) following the manufacturer's instructions in order to remove residual DNA contaminations prior to reverse transcription. Total RNA (70 ng) was reversely transcribed by use of the First Strand cDNA Synthesis Kit (Fermentas) and the supplied random hexamer primers following the manufacturer's instructions. Detection of gene expression was done by RT-PCR with Sawady-Taq DNA polymerase (PeqLab), 1 μL of cDNA, and 0.2 nM of each primer. For gene expression level measurements, real-time RT-PCR was performed on a BioRad iCycler with Biorad iQ-SYBR Green Supermix, 1 μL of cDNA, and 0.2 nM of each primer. The primers used for RT- and for real time RT-PCR (primers 12 and 13, Table 3) anneal within the genes *kdpC* and *cat3*, respectively, and the reaction results in a specific 300-bp PCR product. Both PCRs were carried out using an initial denaturation at 98°C for 3 min, followed by 40 cycles of denaturation at 98°C for 1 min, annealing at 64°C for 30 s, and extension at 72°C for 30 s. In case of real time RT-PCR, the calculated C_t values were normalized against C_t values of reactions using primers annealing within the *rpoAI* gene as a non-regulated housekeeping gene (primers 14 and 15, Table 3). The normalization and the calculation of normalized expression levels were done by use of the Q-Gene software (Simon 2003). All purified RNA samples were treated with DNaseI prior to reverse transcription in order to remove any residual DNA contamination. A reaction with only H_2O and a reaction with DNaseI-treated RNA (without reverse transcription) were included as negative and non-RT-controls, respectively. In case of *H. salinarum* R1 Δ*kdpFABCcat* complemented with either plasmid-encoded *kdpFABC* or *kdpFABCcat3*, gene expression level measurements were

performed as described for the wild-type except that the primers used for the detection of the *kdpFABC* or *kdpFABC cat3* transcript in real time RT-PCR (primers 16 and 17, Table 3) anneal in *kdpA*.

Results

K^+ as a growth-limiting factor for *H. salinarum* R1

In order to elucidate the growth requirements of *H. salinarum* R1 with respect to K^+, cells were cultivated in medium containing 25% (w/v) total salt with varying concentrations of KCl. Cell cultivation followed standard conditions with vigorous shaking under illumination. Although cells were grown in the light, synthesis of bacteriorhodopsin is dependent on oxygen limitation and, thus, repressed under these conditions (Baliga et al. 2001). Growth was observed to occur over a large scale of K^+ concentrations, ranging from 1 mM to 2.5 M. *H. salinarum* R1 exhibited similar growth behavior without notable effects on generation time or maximal stationary growth phase optical density if cultivated in K^+ concentrations of 5 and 50 mM (Fig. 1a). In contrast, if cells were cultivated in the presence of initial K^+ concentrations of 3 mM and below, the stationary growth phase was reached at lower cell densities, arguing for limiting growth conditions due to the lack of K^+. In these cultures, the addition of KCl was sufficient to promote further cell growth, thereby confirming the role of K^+ as the growth-limiting factor. Since *H. salinarum* is able to accumulate high concentrations of potassium ions during growth, the K^+ concentration in the medium is biased by the transport activity of a growing culture. In order to define the K^+ concentrations enabling cell growth, the residual medium K^+ concentration in the stationary growth phase cultures was measured by FEP (Fig. 1b). In all cultures, uptake of K^+ could be observed by means of a decline in the medium K^+ concentration. Cultures grown in the presence of growth-limiting K^+ concentrations (3 and 1 mM) exhibited an identical residual K^+ concentration of 20 μM in the medium. In contrast, in case of cultures with an initial K^+ concentration of 5 and 50 mM, the residual K^+ concentration was found to be 300 μM and 44 mM, respectively, thereby demonstrating that K^+ does not act as a growth-limiting factor. The concentration of 20 μM K^+ in the medium thus represents the maximal K^+ depletion capability of *H. salinarum* R1. Furthermore, these findings demonstrate the presence and activity of high-affinity K^+ uptake systems.

Cellular adaptation to K^+ limitation

In the following, the effect of limiting K^+ concentrations in the medium on the cellular K^+ concentration was analyzed. Cellular K^+ concentrations were measured for cells of the stationary growth phase grown for 8 days as in Fig. 1 with initial medium K^+ concentrations of 100 mM (non-limiting conditions) and 3 mM (limiting conditions). K^+ was analyzed by FEP upon osmotic cell lysis and centrifugation of cell debris. The cellular K^+ concentration was calculated based on the determination of the cell volume (Fig. 2). Cultures grown in the presence of 100 mM potassium comprised a cellular K^+ concentration of approximately 4 M. In contrast, the culture grown with an initial K^+ concentration of 3 mM showed a significantly reduced cellular K^+ concentration of 2.8 M in the stationary phase, which corresponds to a reduction in the internal K^+

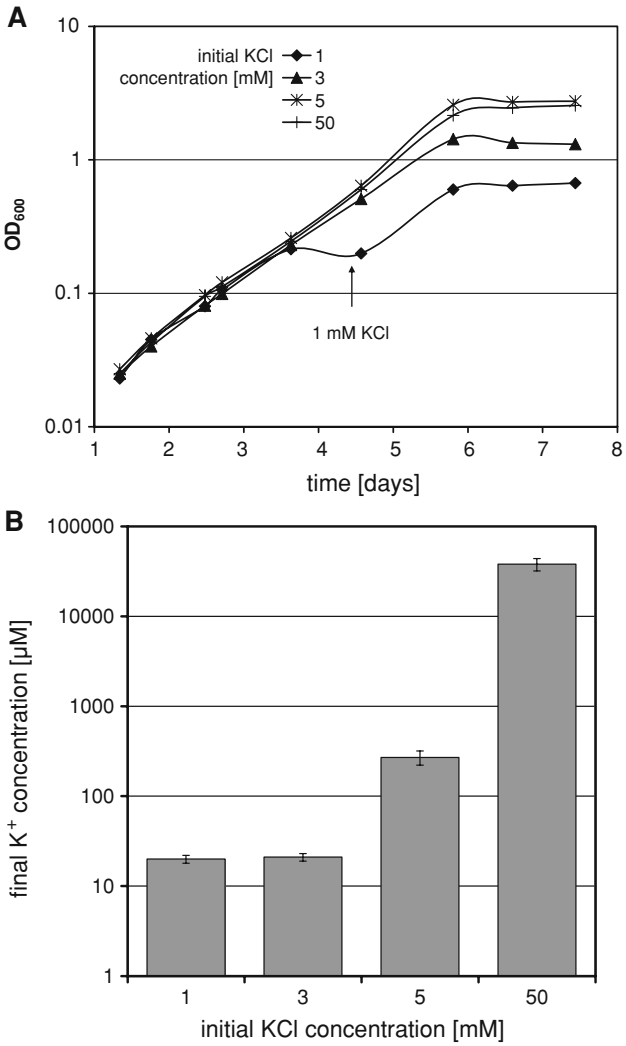

Fig. 1 Cultivation of *H. salinarum* R1 with different initial K^+ concentrations. **a** Growth was monitored as optical density of the culture. Addition of 1 mM of KCl to the culture with an initial K^+ concentration of 1 mM is indicated by an *arrow*. **b** K^+ depletion in the medium caused by growth of *H. salinarum*. Residual medium K^+ concentration was measured by FEP in triplicate from stationary growth phase cultures with different initial K^+ concentrations as indicated

concentration by about 30%. Microscopic analysis of the cells revealed that in parallel to the reduction of the cellular K^+ concentration, the mean volume of the cells was reduced by approx 20 % in case of K^+-limiting conditions. These results indicate that *H. salinarum* R1 is able to down-regulate the intracellular K^+ concentration in response to a reduced availability of K^+ in the medium. Thus, both the activity of high-affinity K^+ uptake systems and a simultaneous reduction of the cellular K^+ concentration allow *H. salinarum* R1 to tolerate very low external K^+ concentrations. In addition, the cell volume is reduced under K^+-limiting conditions. As a consequence, a lower net amount of K^+ is needed to maintain the adapted lower cellular K^+ concentration.

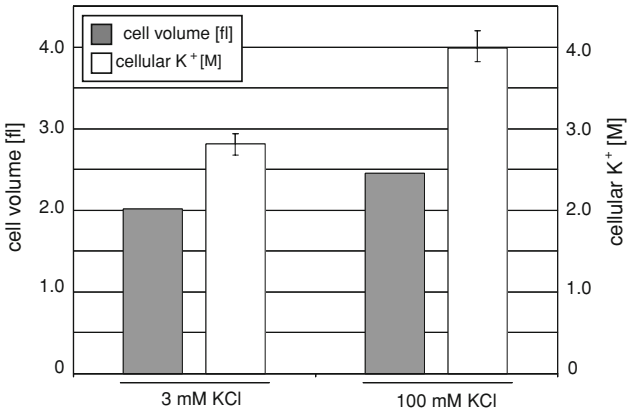

Fig. 2 Cellular K^+ concentration and cell volume of *H. salinarum* R1. Cellular K^+ concentrations and cell volumes were measured from stationary growth phase cultures of *H. salinarum* R1 grown with initial K^+ concentrations of 3 mM (limiting conditions) and 100 mM (non-limiting conditions)

The *kdpFABCcat3* gene cluster as a potential operon

Based on the genome sequences of both *Halobacterium* sp. NRC-1 (Ng et al. 2000) and *H. salinarum* R1 (Pfeiffer et al. 2008), the *kdp* genes are encoded in a gene cluster potentially forming a single operon on one of the smaller extrachromosomal replicons. Here, we try to allocate putative operon and promoter elements within the *kdp* gene cluster based on the DNA sequence of *Halobacterium* sp. NRC-1, where the *kdp* genes are reported to be located on the extrachromosomal replicon pNRC200. Although the reports of Ng et al. (2000) and Pfeiffer et al. (2008) differ with respect on the localization of the *kdp* genes on the different replicons found in these studies, there is no deviation within the DNA sequence of the *kdp* gene cluster between the two strains. It should be emphasized at this point that allocation of operon elements was merely performed by sequence analysis. Thus, our results have to be further verified by experimental analysis, which is going to be published elsewhere. Although the *kdpF* gene has not been annotated as such in the report by Ng et al., our analysis as well as the gene annotation in Pfeiffer et al. (2008) revealed the presence of an ORF preceding the *kdpA* gene, which clearly corresponds to the *kdpF* gene of *E. coli*, thus resulting in a putative *kdpFABCcat3* operon (Fig. 3a). The arrangement of the structural genes *kdpFABC* is identical to the corresponding operon from *E. coli* (Siebers and Altendorf 1993). The *kdp* gene cluster starts with the ORF corresponding to the *kdpF* gene, followed by the genes *kdpA*, *kdpB*, and *kdpC*. No homologs of the bacterial regulatory genes *kdpD* and *kdpE* were found in either *H. salinarum* strain R1 and NRC-1, neither

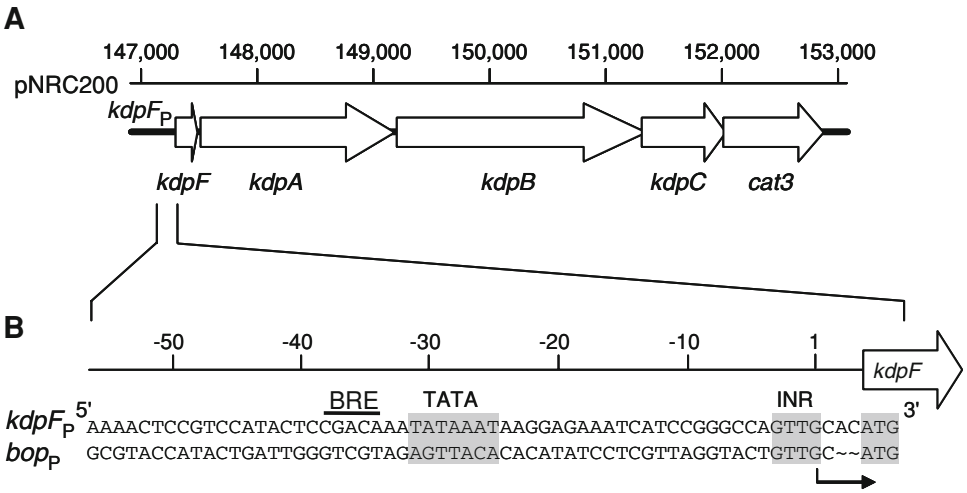

Fig. 3 Organization of the putative *kdpFABCcat3* operon and composition of the deduced promoter. **a** Organization and length of genes within the *kdpFABCcat3* gene cluster. *Numbers* indicate positions on the extrachromosomal replicon pNRC200 according to Ng et al. (2000). **b** Alignment of the *kdpFABCcat3* promotor ($kdpF_P$) to the minimal promotor region of the bacterio-opsin gene (bop_P). The sequence is numbered for bop_P, starting with the transcription start point (*black arrow*) as +1. The translational start codon, transcription initiation region (INR), and TATA-box are shaded. The putative transcription factor TFB binding site (BRE) is marked for $kdpF_P$

organized further downstream in a separate operon directly succeeding *kdpFABC* as in *E. coli*, nor encoded divergently in the opposite direction preceding the structural genes like, for example in *Mycobacterium tuberculosis* (Cole et al. 1998) or anywhere else in the genome. Instead, an additional 819-bp ORF was found downstream of the *kdpC* gene and originally annotated as *cat3* for *H. salinarum* sp. NRC-1 (Ng et al. 2000) and as UspA protein for *H. salinarum* R1 (Pfeiffer et al. 2008). The initial annotation of this ORF as *cat3* originated from its deduced protein sequence similarity to the C-terminal region of the putative amino acid transporter Cat-1 from *Archaeoglobus fulgidus* (Klenk et al. 1997). The deduced proteins Cat3 and Cat-1 comprise only 22% identical residues, which build up a tandem Usp family domain motif in Cat3. This motif is also present in the Cat-1 protein but is not related to its function as amino acid transporter. Based on these findings, the gene product was diversely annotated as UspA protein in *H. salinarum* R1 (Pfeiffer et al. 2008). The annotation as *cat3* is, thus, clearly misleading, and the gene has to be renamed according to its function in the context of the *kdpFABCcat3* genes (see below). However,intergenic distances are very small with only two and one base pairs for *kdpF*/*kdpA* and *kdpA*/*kdpB*, respectively. The genes *kdpB* and *kdpC* as well as *kdpC* and *cat3* do overlap by one base pair. Thus, it is rather unlikely that there are additional promoters in intergenic sequences, which favors the presence of a single *kdpFABCcat3* operon.

The transcription apparatus of Archaea more closely resembles that of Eucarya than that of Bacteria (Woese et al. 1990). This, in turn, leads to a different promoter structure within a putative *kdpFABCcat3* operon with respect to its bacterial counterpart. For an initial analysis, the putative promoter region of the *kdpFABCcat3* gene cluster ($kdpF_P$) was manually aligned to the well-characterized specific 53-bp minimal *bop* promoter (bop_P) (Gropp et al. 1995) (Fig. 3b). In addition, the potential promoter region was compared to more general consensus motifs of haloarchaeal promoters. Whereas in bop_P there is only a weak homology of the TATA box sequence to the common archaeal TATA-box consensus (Baliga and DasSarma 1999), $kdpF_P$ comprises a more distinctive TATA box element TATAAAT(A) corresponding to the common archaeal TATA-box consensus sequence of 5′-T/CTTAT/AA-3′ (Palmer and Daniels 1995). The putative INR element marking the start site of transcription is identical in both bop_P and $kdpF_P$ and resembles the relatively weak consensus of 5′-T/CG/A-3′ (Palmer and Daniels 1995). Thus, for the *kdpFABCcat3* gene cluster, transcription is supposed to start four nucleotides upstream of the ATG start codon from the postulated *kdpF* gene at the G within the GTTG motif. A possible common transcription factor B responsive element (BRE) (Qureshi and Jackson 1998; Soppa 1999) with the sequence CGACA can be found upstream of the TATA-box region in $kdpF_P$, although a distinct BRE cannot be derived from bop_P due to its different specific regulation (Baliga and DasSarma 1999). This location leaves a two base pair distance to the TATA-box, which is similar to the common BRE consensus motif CGAAA followed by two base pairs and the TATA-box (Palmer and Daniels 1995; Brenneis et al. 2007). Thus, $kdpF_P$ carries all conserved *cis*-acting elements required for an active archaeal promoter.

kdpFABCcat3 gene expression

To provide evidence of an active expression of the *kdpFABCcat3* gene cluster, transcription was verified by reverse transcriptase PCR. In order to explore inducing or non-inducing conditions in general, total RNA of *H. salinarum* R1 was purified from a culture grown in rich medium, and the expression of the *kdpFABCcat3* genes was detected by sequence-specific primers annealing in *kdpC* and *cat3* (Fig. 4). The use of genomic DNA as a template revealed the presence of the genes at all and, thus, served as a positive control (lane 1). As a negative control for template purity, no PCR product could be detected with DNaseI-degraded total RNA without reverse transcription (lane 2). In case of reversely transcribed cDNA as template, the specific 300-bp PCR target product could be detected (lane 3), thereby clearly demonstrating the transcription of the corresponding *kdp* genes. Thus, although the Kdp system has so far only been reported to exist in Bacteria, *H. salinarum* R1 encodes and also actively expresses genes homologous to the Kdp system.

kdpFABCcat3 and *kdpFABC* deletion and the effect of *cat3*

In order to study the specific role of the Kdp system and the gene product of *cat3* in the K^+ homeostasis of *H.*

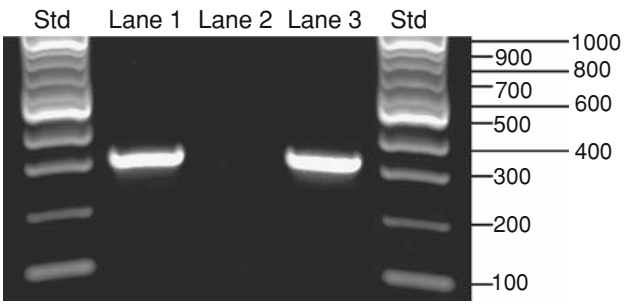

Fig. 4 Detection of gene expression of the *kdpFABCcat3* genes by reverse transcriptase PCR. DNA was amplified with sequence-specific primers binding in *kdpC* and *cat3*. Genomic DNA without DNaseI treatment (lane 1), DNaseI-degraded RNA without reverse transcription (non-RT negative control; lane 2), and cDNA from DNaseI-treated RNA (lane 3) were used as template. *Std* length standard

salinarum, a deletion of both the entire *kdpFABCcat3* gene cluster as well as of only the *kdpFABC* genes was carried out. In case of rich medium with non-limiting K^+ concentrations, the resulting deletion strains exhibited a growth curve identical to the wild-type. In contrast, both deletion strains showed a slightly different growth phenotype with respect to the wild-type in case of K^+ limitation (Fig. 5a). As shown above, *H. salinarum* R1 cultivated in medium with an initial K^+ concentration of 3 mM reached an early stationary growth phase due to K^+-limiting conditions. Both the *kdpFABCcat3* and *kdpFABC* deletion strains comprised a similar growth phenotype during the exponential phase but entered the stationary phase at a lower optical density. Although there is apparently only a slight difference between wild-type and mutant strains, this effect was highly reproducible with an error in the ratio of the final optical densities of less than 5 %. The effect of the *kdpFABCcat3* and *kdpFABC* deletion became more pronounced when the residual K^+ concentration in the stationary growth phase medium was analyzed (Fig. 5b). The wild-type strain was again able to accumulate K^+ down to 20 μM residual [K^+]. In contrast, both the *kdpFABCcat3* and *kdpFABC* deletion strains were only able to grow in the presence of K^+ concentrations above 60 μM, thereby demonstrating that the altered growth phenotype is connected to the deletion of the high-affinity K^+ uptake system under K^+-limiting conditions.

Whereas both deletion strains comprised the same phenotype with respect to the tolerance of K^+ limitation, complementation was strongly dependent on the presence of the *cat3* gene (Fig. 6). The phenotype of the *kdpFABCcat3* deletion strain could completely be restored and, thus, complemented by the concomitant expression of the plasmid-encoded *kdpFABCcat3* genes, whereas the complementation with plasmid-encoded *kdpFABC* without *cat3* did not lead to restoration. These findings suggest an essential role of the *cat3* gene product, either for the activity of the transport complex itself or for the expression of the corresponding genes.

Regulation of *kdpFABCcat3* gene expression

In bacteria, the expression of *kdpFABC* is generally governed by the sensor kinase/response regulator pair KdpD/KdpE and is highly inducible under K^+-limiting conditions, where the KdpFABC complex functions as a high-affinity K^+-scavenging ATPase. In addition, a strong Kdp-dependent K^+ uptake can also be observed in case of a NaCl-mediated osmotic upshock (Jung and Altendorf 2002). For *H. salinarum*, the expression of a high affinity, ATP-dependent Kdp system is feasible under conditions of a low membrane potential (due to ATP-dependency) and/or low medium K^+ concentrations (due to high affinity), both leading to an increasing $\Delta\psi_{K+}$. Under these conditions, the potassium channels and the Trk systems can no longer supply the cell with K^+ due to either energetic and/or affinity considerations.

To obtain information about the regulation of *kdpFABCcat3* expression under K^+-limiting conditions, gene transcription was quantitatively followed by reverse transcriptase (RT) PCR. Expression of the *kdp* genes could already be observed under non-limiting conditions using rich medium (see Fig. 4), but without any quantitative means. In order to analyze the effect of the medium K^+ concentration on the expression rate of the *kdpFABCcat3* gene cluster more precisely, cells were cultivated in the presence of different initial K^+ concentrations (3, 5, and 50 mM KCl) (Fig. 7). K^+ uptake was followed by FEP (Fig. 7a), and the expression rate of the *kdpFABCcat3* genes was concomitantly measured quantitatively by real-time RT-PCR (Fig. 7b). As expected, in a culture grown in non-limiting K^+ concentrations of 50 mM KCl, gene expression is on a low but still detectable constitutive level, which is in accord with the transcript analysis by reverse

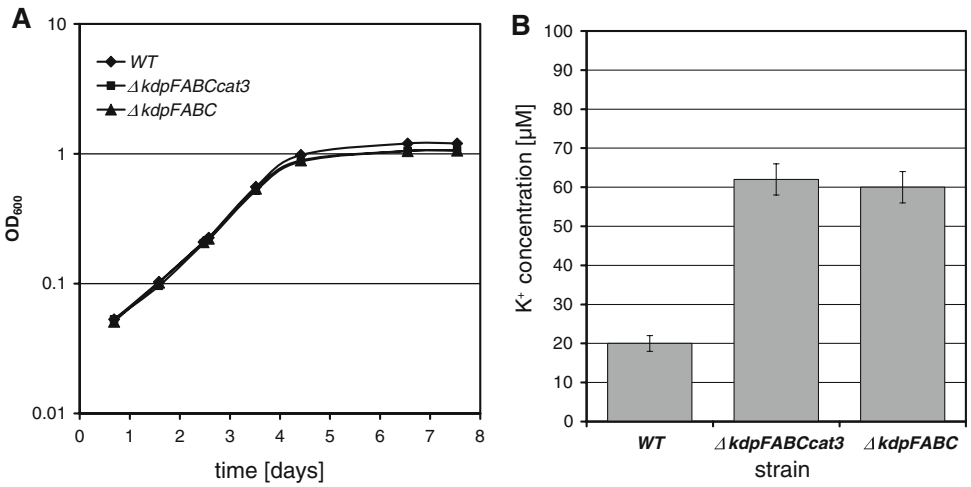

Fig. 5 Phenotype of the deletion of *kdpFABCcat3* and *kdpFABC*. **a** Cultivation of *H. salinarum* R1, *H. salinarum* R1 Δ*kdpFABCcat3*, and *H. salinarum* R1 Δ*kdpFABC* in media initially containing 3 mM KCl. The growth curves of *H. salinarum* R1 Δ*kdpFABCcat3* and *H. salinarum* R1 Δ*kdpFABC* are virtually congruent. **b** Residual medium K^+ concentration measured by FEP in triplicate from stationary growth phase cultures of (**a**)

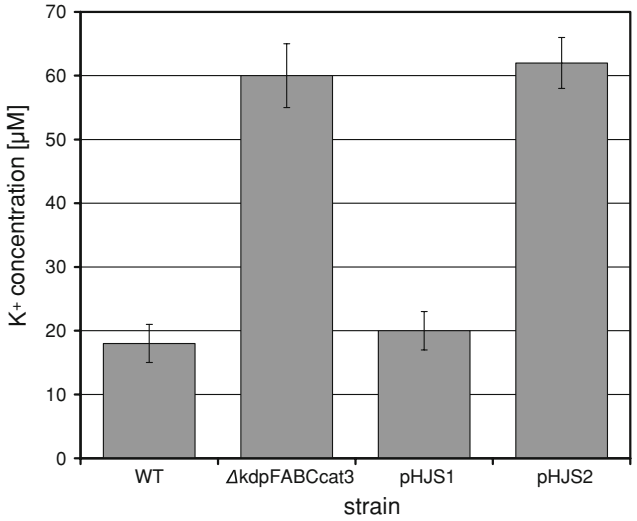

Fig. 6 : Effect of the *cat3* deletion on K^+ uptake. The phenotype of a chromosomal *kdpFABCcat3* deletion was complemented by plasmid-encoded expression of *kdpFABCcat3* (pHJS1) and *kdpFABC* (pHJS2). Residual medium K^+ concentrations were measured by FEP in triplicate from stationary growth phase cultures. WT, wild-type

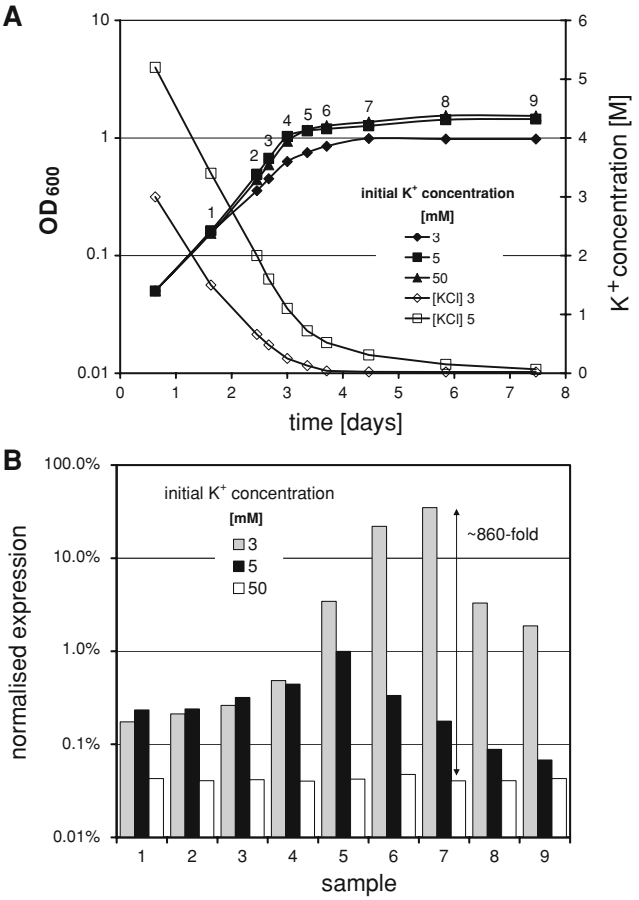

Fig. 7 Quantitative analysis of K^+-dependent growth and K^+-induced *kdpFABCcat3* gene expression. **a** Cultivation of *H. salinarum* R1 in media containing different initial K^+ concentrations was monitored as optical density of the culture (left *y*-axis). Residual medium K^+ concentration was measured by FEP for cultures grown at an initial K^+ concentration of 3 mM and 5 mM (right *y*-axis). Samples were collected from all cultures for real time RT-PCR analysis and are numbered corresponding to sample numbers of (**b**). **b** Normalized expression levels of *kdpFABCcat3* were measured by real time RT-PCR in media containing initial K^+ concentrations of 3, 5, and 50 mM

transcriptase PCR in rich medium. In contrast, in cultures grown in 5 and 3 mM of KCl (i.e., K^+ limitation), a very high transcript level was found. The level of expression was clearly dependent on the initial K^+ concentration in the medium and reached its maximum in the culture grown with 3 mM KCl at the lowest medium K^+ concentration, which is 20 µM (sample 7). At that point, the *kdp* gene cluster is almost 1000-fold induced with respect to the low constitutive expression level in the presence of 50 mM KCl in medium. From this experiment, the dependence of gene expression, residual K^+ concentration in the stationary growth phase, and K^+-limiting growth conditions becomes evident: Maximal gene expression occurs in case of extremely low external K^+ concentrations, which, in turn, lead to an earlier stationary growth phase. The culture grown in 5 mM KCl still did not comprise a stationary K^+ depletion level in the medium, which is in accord with the comparably reduced expression rate of the *kdp* genes with respect to the culture grown in 3 mM KCl. Only in case of 3 mM initial KCl, the cells reached the minimal K^+ concentration enabling growth and, hence, enter the stationary phase due to K^+ depletion with a maximum in *kdpFABCcat3* expression.

Function of *cat3*

As demonstrated by the experiments shown in Fig. 6, expression of plasmid-encoded *kdpFABCcat3* was sufficient to complement the phenotype of a chromosomal *kdpFABCcat3* deletion strain, whereas expression of only *kdpFABC* was not. This readily identified *cat3* as an essential component of the halobacterial Kdp system. In order to study whether Cat3 is involved in the transcriptional regulation of the *kdpFABCcat3* genes or in the formation of the transport complex itself, the complementation assay was analyzed in more detail. The expression of plasmid-encoded *kdpFABCcat3* (pHJS1) and *kdpFABC* (pHJS2) was studied in a *kdpFABCcat3* deletion background with real-time RT-PCR (Fig. 8). Both strains were cultured in media containing 3 or 100 mM KCl, and samples were collected in the late exponential growth phase ($OD_{600} \approx 1$). The complementation with plasmid-encoded *kdpFABCcat3* was found to be comparable to the wild-type, with the same maximum induction rate in the presence of limiting K^+ concentrations, together with a low constitutive expression level in case of non-limiting

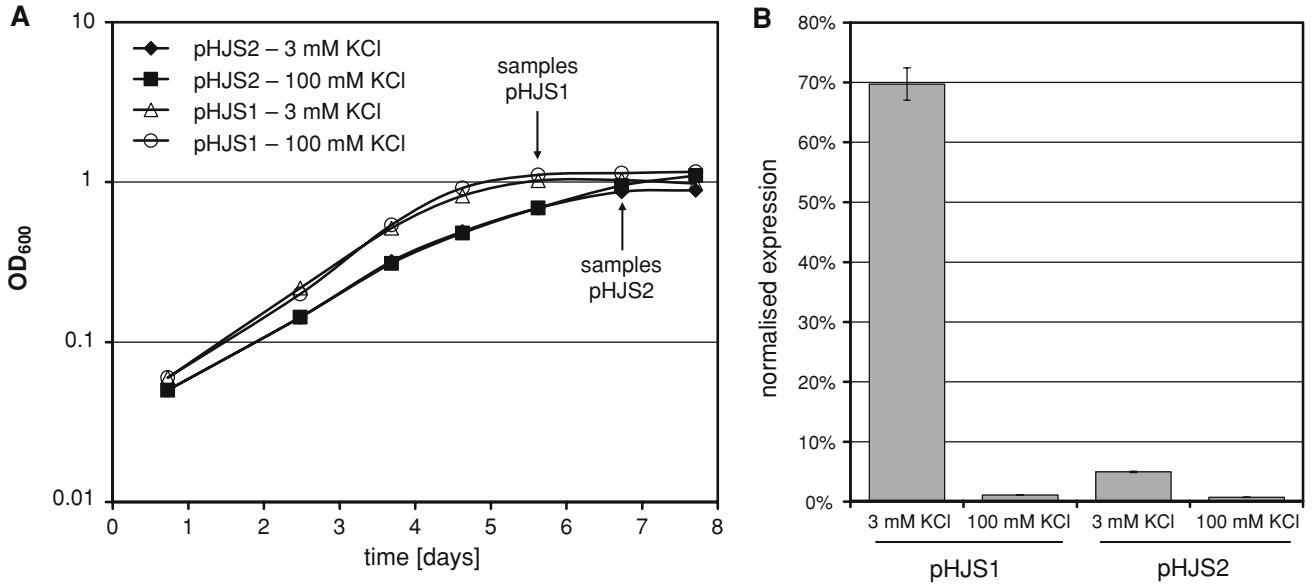

Fig. 8 Function of Cat3 in the transcriptional regulation of the *kdpFABCcat3* genes. **a** Complementation of *H. salinarum* R1 Δ*kdpFABCcat3* with plasmids pHJS1 (*kdpFABCcat3*) and pHJS2 (*kdpFABC*Δ*cat3*) in media containing 3 and 100 mM initial K^+, monitored as optical density of the culture. **b** Normalized expression levels of *kdpFABC* gene expression in the late exponential growth phase as measured by real time RT-PCR in triplicate

100 mM KCl. In contrast, complementation with only *kdpFABC* resulted in a significantly lower induction level (<10%) even in case of limiting K^+ concentrations, whereas no differences were observed in case of 100 mM KCl. Based on these results, the *cat3* gene product is most likely not involved in the formation of the transport complex itself but has an essential function in the transcriptional regulation in *kdpFABCcat3* gene expression. As already mentioned, the annotation of *cat3* as a cationic amino acid transporter is definitely misleading. Based on our results, we propose the re-naming of the halobacterial *cat3* according to its function in the transcriptional regulation of *kdpFABCcat3* as to *kdpQ*.

Discussion

H. salinarum R1 exhibits a high tolerance with respect to the environmental potassium concentration supporting growth, although K^+ is of vital importance for the cell's life. Even though K^+ is accumulated inside the cell in a molar range, we found that growth occurs in case of very low medium K^+ concentrations of down to >20 μM. We also demonstrated that *H. salinarum* R1 adapts to these conditions by a decrease in both the cellular K^+ concentration as well as the cell volume, which enables the culture to accomplish higher cell densities. Shifts in the cellular K^+ concentration have long been known to occur as a result of changes in illumination conditions, but not as a response to K^+ depletion (Wagner et al. 1978; Lanyi 1978). During illumination, K^+ was shown to reversibly accumulate in high concentrations most probably as a result of the increased membrane potential generated by the activity of the light-driven proton pump bacteriorhodopsin. Thus, both the origin and the direction of the K^+ shift are different from that observed in our study. However, since *H. salinarum* steadily maintains an iso-osmotic equilibrium with the medium (Oren 1999), the lower cellular K^+ level in case of low medium K^+ concentrations is most likely compensated by a concomitantly increased uptake of Na^+. In our studies, the decrease in the cellular K^+ concentration to a stationary value of about 70% with respect to the non-limited high potassium level appears to represent the minimal internal K^+ threshold *H. salinarum* R1 can tolerate. The most likely reason for this effect could reside in the specific adaptation of halophilic proteins to high salt conditions. Most proteins of *H. salinarum* exhibit their activity only in the presence of molar concentrations of Na^+ or K^+ (Kennedy et al. 2001; Madern et al. 2000; Elcock and McCammon 1998). Since K^+ is the dominant cation in the cytoplasm of *H. salinarum*, the presence of a minimum cellular K^+ concentration supporting activity of at least many essential proteins is feasible. NaCl-saturated salt brines comprise a water activity (a_W) of 0.75. Saturated KCl, in contrast, features an a_W value of 0.86, resulting in significantly more free water molecules due to less coordination events. If now, under conditions of K^+ limitation, the internal K^+ concentration is decreased by approx. 30%

(i.e., from 4 M to about 2.8 M), this 30% in K^+ is replaced by Na^+, which readily leads to a significant loss in internal water molecules in order to coordinate the increasing Na^+. As a consequence, proteins are supposed to release low entropy surface water, which may have a great impact on protein structure and function. The presence of a minimal cellular K^+ concentration, which cannot be substituted by Na^+, would, in turn, have a drastic effect on the physiology and ecology of the organism. Since *H. salinarum* is in iso-osmotic equilibrium with the environment, a decline in the external salinity should result in an accordingly reduced concentration of K^+ and Na^+ inside the cell. If the external salinity decreases below the internal minimal threshold for potassium, this would result in an elevated hydrostatic pressure and in cell lysis. Thus, a minimal intracellular K^+ threshold primarily determines the lower level of salt tolerance. This view is supported by the fact that the value of around 2.8 M internal K^+ found in our studies is well in accord with the lower limit of salt tolerance reported for *H. salinarum*.

Our analyses revealed that the halobacterial Kdp system is essential for growth in case of K^+ concentrations below 60 μM, and under these conditions, the corresponding genes *kdpFABCcat3* are highly expressed. Expression is induced by a decline of the medium K^+ concentration with highest levels near limiting K^+ concentrations of below 200 μM. These findings are in good accord with the reported characteristics of bacterial Kdp systems (Jung and Altendorf 2002). Also in *E. coli*, the deletion of the *kdp* genes results in an elevated minimal K^+ concentration enabling growth. At first glance, these results support the notion that the Kdp complex of *H. salinarum* is used accordingly as a high-affinity K^+ uptake system, which is induced under conditions, in which either affinity and/or driving force of other K^+ uptake systems are not sufficient to facilitate K^+ uptake. Thus, our report demonstrates for the first time a medium K^+-dependent expression of an ATP-consuming high-affinity potassium transport complex in a *H. salinarum* strain. Apparently, the only benefit of the Kdp system found in our studies is a further decrease of 40 μM in the minimal K^+ concentration enabling growth of cells, which normally thrive under conditions of above 100 mM potassium. However, it should be noted that the aim of our studies was to demonstrate that there is an ATP-driven transporter and not why there is an ATP-driven transporter. In addition, here we only studied the response of *H. salinarum* R1 to K^+ limitation. Further investigations are needed in order to analyze the influence of $\Delta\psi_m$ as a possible inducing factor. However, both a decrease in $\Delta\psi_m$ and external K^+ limitation would initially lead to a decrease in the intracellular K^+ level due to insufficient K^+ uptake via the potassium channel proteins. Thus, both initial stimuli merge in the same effect and serve as the primary stimulus for *kdpFABCcat3* expression.

In Bacteria, *kdpFABC* expression is normally governed by response to high osmolality and K^+ limitation. Since *Halobacterium* is osmotically balanced with its environment, the KdpFABC complex is not required to be involved in turgor regulation and, hence, there is no need for an appropriate complex sensory system analogous to the *E. coli* KdpD/KdpE sensor kinase/response regulator framework. In addition, the KdpE protein of *E. coli* serves as a transcriptional activator binding to the DNA via a typical bacterial helix-turn-helix motif. The fact that haloarchaea comprise an essentially different transcriptional apparatus, in which a putative KdpE homolog would have to interact with transcription factors, TATA-box binding proteins and different RNA polymerases, renders the presence of a closely related polypeptide rather unlikely. However, the deduced Cat3 protein consists of a tandem Usp domain motif with no further domains or extensions. Usp domains share a common three-dimensional protein fold and are frequently found in stress-induced regulatory proteins. They can be subdivided by their ATP binding properties (Aravind et al. 2002). Cat3 could at least in part correspond to the bacterial KdpD, since it closely resembles a structural pattern of the N-terminal part of KdpD ($KdpD_{251–372}$), for which a potential Usp domain structure as well as a regulatory effect of ATP binding have already been reported (Heermann et al. 2000; Aravind et al. 2002). A functional homology of Cat3 and $KdpD_{251–372}$ is further favored by the fact that the N-terminal domain of KdpD bearing the Usp motif is rather unique and cannot be found in any other sensor kinase proteins sequenced so far (Jung and Altendorf 2002). Thus, also Cat3 could work as a possible ATP-activated molecular switch, although typical DNA-binding regulatory properties are rather unlikely since there is no structural homology to any known DNA binding motif. The *cat3* gene product was found to be essential for the induced expression of the *kdpFABCcat3* genes. If Cat3 does not exert its regulatory function at the level of the DNA, at least one additional regulator has to be present in order to trigger gene transcription. Nevertheless, the current opinion that K^+ homoeostasis is solely mediated passively via membrane potential-driven K^+ uniporters is only one aspect of a more complex system.

Acknowledgments The authors kindly acknowledge Karlheinz Altendorf as well as the Arbeitsgruppe Mikrobiologie (Universität Osnabrück) for generous scientific and financial support. Ursula Krehe is acknowledged for excellent technical assistance. Dieter Oesterhelt and Jörg Tittor are kindly acknowledged for valuable scientific discussion as well as for the kind donation of plasmid pMKK100. H. S. was supported by the Boehringer Ingelheim Fonds.

References

Aravind L, Anantharaman V, Koonin EV (2002) Monophyly of class I aminoacyl tRNA synthetase, USPA, ETFP, photolyase, and PP-ATPase nucleotide-binding domains: implications for protein evolution in the RNA. Proteins 48:1–14

Bakker EP (1993) Low-affinity K^+ uptake systems. In: Bakker EP (ed) Alkali cation transport systems in prokaryotes. CRC Press Inc, Boca Raton, pp 253–276

Baliga NS, DasSarma S (1999) Saturation mutagenesis of the TATA box and upstream activator sequence in the haloarchaeal *bop* gene promoter. J Bacteriol 181:2513–2518

Baliga NS, Kennedy SP, Ng WV, Hood L, DasSarma S (2001) Genomic and genetic dissection of an archaeal regulon. Proc Natl Acad Sci USA 98:2521–2525

Bramkamp M, Altendorf K, Greie J-C (2007) Common patterns and unique features of P-type ATPases: a comparative view on the KdpFABC complex from *Escherichia coli*. Mol Membr Biol 24:375–386

Brenneis M, Hering O, Lange C, Soppa J (2007) Experimental characterization of *Cis*-acting elements important for translation and transcription in halophilic archaea. PLoS Genet 3:e229

Cline SW, Lam WL, Charlebois RL, Schalkwyk LC, Doolittle WF (1989) Transformation methods for halophilic archaebacteria. Can J Microbiol 35:148–152

Cole ST, Brosch R, Parkhill J, Garnier T, Churcher C, Harris D et al (1998) Deciphering the biology of *Mycobacterium tuberculosis* from the complete genome sequence. Nature 393:537–544

Elcock AH, McCammon JA (1998) Electrostatic contributions to the stability of halophilic proteins. J Mol Biol 24:731–748

Greie J-C, Altendorf K (2007) The K^+-translocating KdpFABC complex from *Escherichia coli*: a P-type ATPase with unique features. J Bioenerg Biomembr 39:397–402

Gropp F, Gropp R, Betlach MC (1995) Effects of upstream deletions on light- and oxygen-regulated bacterio-opsin gene expression in *Halobacterium halobium*. Mol Microbiol 16:357–364

Guzman LM, Belin D, Carson MJ, Beckwith J (1995) Tight regulation, modulation, and high-level expression by vectors containing the arabinose pBAD promoter. J Bacteriol 177:4121–4130

Heermann R, Altendorf K, Jung K (2000) The hydrophilic N-terminal domain complements the membrane-anchored C-terminal domain of the sensor kinase KdpD of *Escherichia coli*. J Biol Chem 275:17080–17085

Jung K, Altendorf K (2002) Towards an understanding of the molecular mechanisms of stimulus perception and signal transduction by the KdpD/KdpE system of *Escherichia coli*. J Mol Microbiol Biotechnol 4:223–228

Kauri T, Wallace R, Kushner DJ (1990) Nutrition of the halophilic archaebacterium, *Haloferax volcanii*. Syst Appl Microbiol 13:14–18

Kennedy SP, Ng WV, Salzberg SL, Hood L, DasSarma S (2001) Understanding the adaptation of *Halobacterium* species NRC-1 to its extreme environment through computational analysis of its genome sequence. Genome Res 11:1641–1650

Klenk HP, Clayton RA, Tomb J-F, White O, Nelson KE, Ketchum KA et al (1997) The complete genome sequence of the hyperthermophilic, sulphate-reducing archaeon *Archaeoglobus fulgidus*. Nature 390:364–370

Koch MK, Oesterhelt D (2005) MpcT is the transducer for membrane potential changes in *Halobacterium salinarum*. Mol Microbiol 55:1681–1694

Kokoeva MV, Storch KF, Klein C, Oesterhelt D (2002) A novel mode of sensory transduction in archaea: binding protein-mediated chemotaxis towards osmoprotectants and amino acids. EMBO J 15:2312–2322

Krebs MP, Mollaaghababa R, Khorana HG (1993) Gene replacement in *Halobacterium halobium* and expression of bacteriorhodopsin mutants. Proc Natl Acad Sci USA 90:1987–1991

Lanyi JK (1978) Light energy conversion in *Halobacterium halobium*. Microbiol Rev 42:682–706

Lanyi JK, Helgerson SL, Silverman MP (1979) Relationship between proton motive force and potassium ion transport in *Halobacterium halobium* envelope vesicles. Arch Biochem Biophys 193:329–339

Madern D, Ebel C, Zaccai G (2000) Halophilic adaptation of enzymes. Extremophiles 4:91–98

Meury J, Kohiyama M (1989) ATP is required for K^+ active transport in the archaebacterium *Haloferax volcanii*. Arch Microbiol 151:530–536

Michel H, Oesterhelt D (1980) Electrochemical proton gradient across the cell membrane of *Halobacterium halobium*: effect of *N*,*N*′-dicyclohexylcarbodiimide, relation to intracellular adenosine triphosphate, adenosine diphosphate, and phosphate concentration, and influence of the potassium gradient. Biochemistry 19:4607–4614

Nakamura T, Yamamuro N, Stumpe S, Bakker EP (1998) Cloning of the *trkAH* gene cluster and characterization of the Trk K^+-uptake system of *Vibrio alginolyticus*. Microbiology 144:2281–2289

Ng WV, Kennedy SP, Mahairas GG, Berquist B, Pan M, Shukla HD et al (2000) Genome sequence of *Halobacterium* species NRC-1. Proc Natl Acad Sci USA 97:12176–12181

Oren A (1999) Bioenergetic aspects of halophilism. Microbiol Mol Biol Rev 63:334–348

Palmer JR, Daniels CJ (1995) In vivo definition of an archaeal promoter. J Bacteriol 177:1844–1849

Palmgren MG, Axelsen KB (1998) Evolution of P-type ATPases. Biochim Biophys Acta 1365:37–45

Pfeiffer F, Schuster SC, Broicher A, Falb M, Palm P, Rodewald K, Ruepp A et al (2008) Evolution in the laboratory: the genome of *Halobacterium salinarum* strain R1 compared to that of strain NRC-1. Genomics 91:335–346

Qureshi SA, Jackson SP (1998) Sequence-specific DNA binding by the *S. shibatae* TFIIB homolog, TFB, and its effect on promoter strength. Mol Cell 1:389–400

Roberts MF (2005) Organic compatible solutes of halotolerant and halophilic microorganisms. Saline Systems 1:5

Sambrook J, Fritsch EF, Maniatis T (2001) Molecular cloning: a laboratory manual, 3rd edn. Cold Spring Harbor Laboratory Press, Cold Spring Harbor

Siebers A, Altendorf K (1993) K^+-translocating Kdp-ATPases and other bacterial P-type ATPases. In: Bakker EP (ed) Alkali cation transport systems in prokaryotes. CRC Press Inc, Boca Raton, pp 225–252

Simon P (2003) Q-Gene: processing quantitative real-time RT-PCR data. Bioinformatics 22:1439–1440

Soppa J (1999) Transcription initiation in Archaea: facts, factors and future aspects. Mol Microbiol 31:1295–1305

Stoeckenius W, Kunau WH (1968) Further characterization of particulate fractions from lysed cell envelopes of *Halobacterium halobium* and isolation of gas vacuole membranes. J Cell Biol 38:337–357

Stumpe S, Schlösser A, Schleyer M, Bakker EP (1996) K^+ circulation across prokaryotic cell membrane: K^+ uptake systems. In: Konings WN, Kaback HR, Lolkema JS (eds) Handbook of biological physics, vol 2. Elsevier, Amsterdam, pp 473–499

Wagner G, Hartmann R, Oesterhelt D (1978) Potassium uniport and ATP synthesis in *Halobacterium halobium*. Eur J Biochem 89:169–179

Woese CR, Kandler O, Wheelis ML (1990) Towards a natural system of organisms: proposal for the domains Archaea, Bacteria, and Eucarya. Proc Natl Acad Sci USA 87:4576–4579